Crystal Structure and Thermal Solid-State Reactivity of Ammonium Cyanoureate $NH_4[H_2NC(=O)NCN]$

Bettina V. Lotsch and Wolfgang Schnick

Department Chemie und Biochemie, Lehrstuhl für Anorganische Festkörperchemie,
Ludwig-Maximilians-Universität München, Butenandtstraße 5-13, D-81377 München, Germany

Reprint requests to Prof. Dr. W. Schnick. Fax +49-89-2180-77440.
E-mail: wolfgang.schnick@uni-muenchen.de

Z. Naturforsch. **59b,** 1229 – 1240 (2004); received July 30, 2004

Dedicated to Professor Hubert Schmidbaur on the occasion of his 70th birthday

The ammonium salt of cyanourea $NH_4[H_2NC(=O)NCN]$ has been synthesised *via* an acid-base route from the parent acid and characterized by single-crystal and powder X-ray diffraction, NMR and vibrational spectroscopy, mass spectrometry as well as thermal analysis. The molecular salt ($P2_1/c$, $a = 388.95(8)$, $b = 1121.0(2)$, $c = 1096.4(2)$ pm, $\beta = 92.57(3)^\circ$, $V = 477.5(2)\cdot10^6$ pm^3, $Z = 4$, $T = 140$ K) which may formally be derived from the related compound ammonium dicyanamide $NH_4[N(CN)_2]$ by addition of one molecule water, consists of isolated ammonium and cyanoureate ions which are assembled *via* H···N and H···O hydrogen bonds, forming a three-dimensional arrangement. At elevated temperatures, ammonium cyanoureate undergoes a complex transformation affording the formation of urea and cyanoguanylurea $H_2NC(=O)NHC(NH_2)=NCN$ or the isomeric ammeline $(C_3N_3)(NH_2)_2(OH)$ as the main products, depending on the reaction conditions. The transformation is accompanied by consecutive reactions such as proton transfer and the dis- and reassembly of molecular fragments, yielding a macroscopic segregation of the reaction products. The conversion represents yet another example of a complex reaction proceeding in the solid-state.

Key words: Solid-State Reaction, Crystal Structure, Cyanourea, Thermal Reactivity

Introduction

The detailed investigation of reaction mechanisms has largely been the domain of solution chemistry, owing partly to a large number of degrees of freedom and the resulting direct and facile reaction pathways, and to the well-established routine techniques such as solution NMR available for studying reactions *in situ*. As a consequence, a number of reactions of major importance, such as the historic conversion of ammonium cyanate into urea, have been investigated thoroughly in the liquid phase, yet only very little attention has been directed towards the solid-phase behaviour of the reactants [1 – 3]. Substantial progress concerning solid-state reactivity has been achieved by the systematic investigation of photoreactions such as [2+2] monomolecular and bimolecular photodimerizations, which often exhibit single-crystal-to-single-crystal character [4]. However, satisfactory insight into the mechanisms of thermally induced solid-state reactions is still rare.

In order to close this gap, we have started a systematic investigation of molecular solids that may be envisioned empirically as possible candidates for exhibiting solid-state reactivity due to their molecular and crystal structures. On this background, we have been focussing particularly on dicyanamide salts, whose solid-phase reactivity is largely driven by the respective counter ions and which, therefore, provide a versatile and tuneable system for the study of solid-state reactions [5 – 8].

In this context, ammonium dicyanamide (**2**), whose reactivity may be understood by a simple isolobal analogy with Wöhler's classic synthesis of urea, has turned out to be a particularly suitable model system in terms of temperature, kinetics, purity, and completeness of the transformation [9, 10]. When heated to temperatures above 353 K, the ionic ammonium dicyanamide $NH_4[N(CN)_2]$ is converted into its molecular isomer dicyandiamide $(H_2N)_2C{=}NCN$ in a topochemical solid-state reaction [10 – 12]. Due to the fundamental role of the ammonium ion and the nitrile-group of the

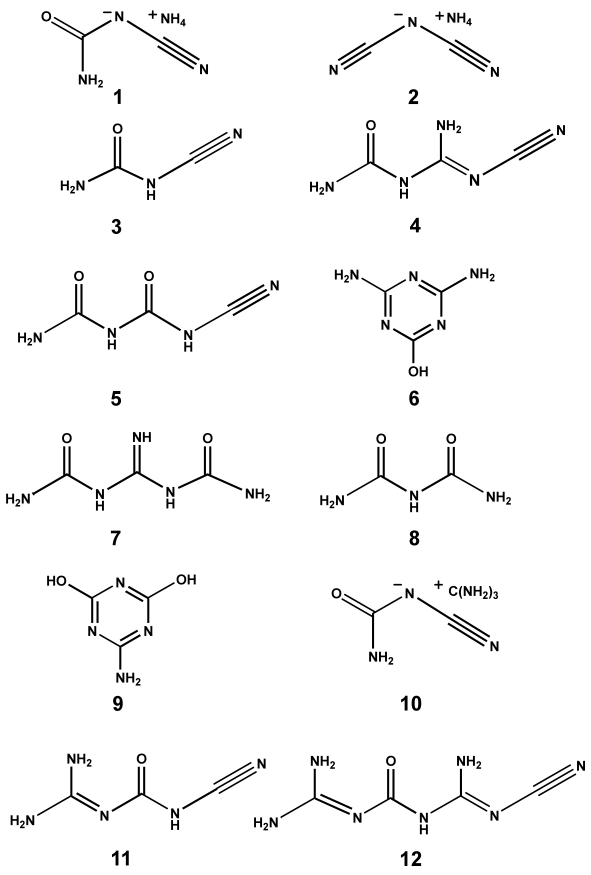

Scheme 1. Molecular formulas of several compounds which are chemically or structurally related to the cyanourea structure: (**1**) ammonium cyanoureate, (**2**) ammonium dicyanamide, (**3**) cyanourea, (**4**) cyanoguanylurea, (**5**) cyanobiuret, (**6**) ammeline, (**7**) 1,3-dicarbamoylguanidine, (**8**) biuret, (**9**) ammelide, (**10**) guanidinium cyanoureate, (**11**) cyanocarbamoylguanidine, (**12**) [1-cyanoguanyl-3-guanyl]urea.

Table 1. Crystal data and structure refinement of $NH_4[H_2NC(=O)NCN]$.

Empirical formula	$C_2\,H_6\,N_4\,O$
Molar mass [g·mol^{-1}]	102.11
Crystal system	monoclinic
Space group	$P2_1/c$ (no. 14)
T [K]	140
Diffractometer, monochromator	STOE STADI 4, graphite
Radiation [λ / pm]	Mo-K$_\alpha$ (71.073)
Z	4
a [pm]	388.95(8)
b [pm]	1121.0(2)
c [pm]	1096.4(2)
β [°]	92.57(3)
V [10^6·pm^3]	477.5(2)
Calculated density [g·cm^{-3}]	1.420
Crystal size [mm^3]	$0.51 \times 0.29 \times 0.18$
Absorption coefficient [mm^{-1}]	0.115
Scan type	ω
$F(000)$	216
Diffraction range [°]	$2.60 \le \theta \le 28.02$
Index range	$-5 \le h \le 5$, $-14 \le k \le 14$, $-14 \le l \le 14$
Total no. reflections	6513
Independent reflections	1158
Observed reflections	980 ($R_{int} = 0.0360$)
Refined parameters / constraints	89 / 0
Corrections	Lorentz, absorption, polarisation, extinction
GOF on F^2	1.073
Final R indices $\lvert I > 2\sigma(I)\rvert$	$R1 = 0.0297$ $wR2 = 0.0769$
R Indices (all data)	$R1 = 0.0397$ $wR2 = 0.0829$ with $w = [\sigma^2({F_o}^2) + (0.0409P)^2 + 0.1113P]^{-1}$ where $P = ({F_o}^2 + 2{F_c}^2)/3$
Min./max. residual electron density [e·Å^{-3}]	−0.193 / 0.203

dicyanamide anion in this transformation, comparable systems with similar reactive groups were devised in order to address the question whether or not a core framework of molecular and structural presuppositions may be established, which underlies and directs the observed type of solid-state reactivity.

Among the potential candidates, ammonium cyanoureate (**1**) was found to be quite closely related to ammonium dicyanamide (**2**), from which it can formally be derived by addition of H_2O to one of the nitrile-groups, thereby maintaining the ammonium ion and one nitrile-group as the reactive centres. Although the free acid cyanourea (N-cyanocarbamimidic acid) (**3**) has been mentioned as early as 1870 in the literature [13] and its molecular structure and reactivity has been characterized [14 – 17], crystal structure information is only available for the silver and, though incomplete, for the potassium salt of cyanourea [18, 19]. Studies on the behaviour of cyanourea in aqueous and organic solution reveal the susceptibility of cyanourea to intermolecular addition and consecutive decomposition reactions. In neutral and organic solution, different degrees of cyanoguanylurea (**4**) and cyanobiuret (**5**) are formed [20], whereas ammeline (**6**) (2,4-amino-6-hydroxy-1,3,5-triazine) and 1,3-dicarbamoylguanidine (**7**) are the main products in alkaline and acidic solution, respectively (Scheme 1) [21, 22].

On the background of our ongoing studies of the mechanistic aspects of solid-state reactions we are interested in the structure-reactivity relations of ammo-

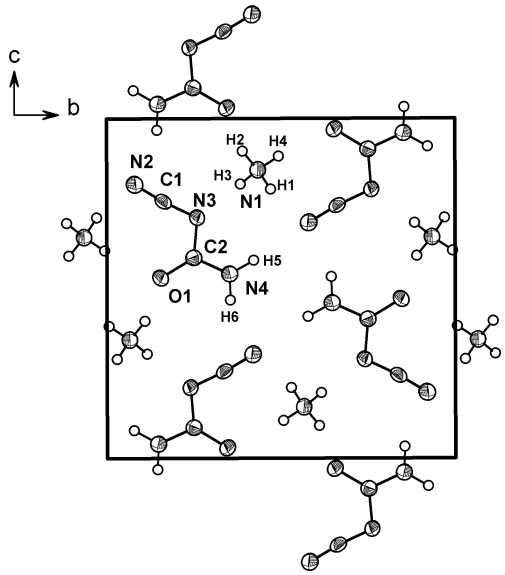

Fig. 1. Crystal structure of $NH_4[H_2NC(=O)NCN]$, view along [100]. Ellipsoids are drawn at the 70% probability level.

nium cyanoureate in the solid phase. In this contribution we report on the synthesis, characterization and X-ray crystal structure of ammonium cyanoureate as well as its solid-state reactivity as compared to ammonium dicyanamide.

Results

Crystal structure

Ammonium cyanoureate crystallizes in the space group $P2_1/c$ (no. 14) with four formula units in the monoclinic unit cell. The anions are stacked in parallel chains along [001], forming a framework in which pairs of ammonium ions are embedded (Fig. 1).

As observed in the silver salt of cyanourea [18], the molecular structure of the essentially planar cyanourea anions exhibits a *cisoid* arrangement of the nitrile group and the oxygen atom, rendering the amide group *trans* to the nitrile moiety. The central nitrogen atom carries the negative charge without significant delocalisation into the nitrile group, which is consistent with the interatomic distances N2-C1 116.5 pm and C1-N3 130.7, corresponding to the localisation of the triple bond and, hence, to the molecular formula $N{\equiv}C\text{-}N\text{-}C(=O)NH_2$ for the cyanoureate anion (Table 2).

The anions are hydrogen bonded *via* weak N2···H6 contacts (241.8 pm) between adjacent amide and nitrile groups along [001], and *via* medium strong N2···H5 contacts (216.1 pm) along [001], [0$\bar{1}$1] and [011].

Table 2. Bond lengths (pm) and angles (°) for $NH_4[H_2NC(=O)NCN]$.

O1-C2	125.7(2)	N4-C2	133.8(2)
N4-H5	90(2)	N4-H6	89(2)
N2-C1	116.5(2)	C1-N3	130.7(2)
N1-H1	95(2)	N1-H2	92(2)
N1-H3	91(2)	N1-H4	91(2)
N3-C2	137.5(2)		
C2-N4-H5	121(1)	C2-N4-H6	120(1)
H5-N4-H6	118(2)	N2-C1-N3	174.7(1)
H1-N1-H2	109(2)	H1-N1-H3	108(2)
H2-N1-H3	109(2)	H1-N1-H4	108(2)
H2-N1-H4	110(2)	H3-N1-H4	113(2)
C1-N3-C2	115.61(9)	O1-C2-N4	121.9(1)
O1-C2-N3	123.90(9)	N4-C2-N3	114.23(9)
Hydrogen bonding			
N1-H1…N2	200(2)	N1-H1-N2	167(2)
N1-H2…O1	191(2)	N1-H2-O1	163(2)
N1-H3…N3	199(2)	N1-H3-N3	170(2)
N1-H4…O1	203(2)	N1-H4-O1	157(2)

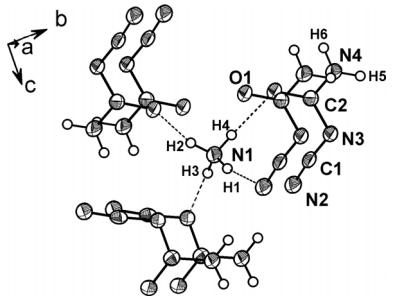

Fig. 2. Coordination sphere of the ammonium ion in $NH_4[H_2NC(=O)NCN]$. The hydrogen bonding network is indicated by dotted lines. Ellipsoids are drawn at the 70% probability level.

The ammonium ion exhibits slight deviations from the ideal tetrahedral symmetry with H-N-H bond angles between 108 and 113° (Table 2). The cation is coordinated by three pairs of anions, of which one pair is doubly coordinated *via* O1 and N2, forming an inner coordination sphere that resembles an irregular heptahedron. The six closest cation(N1)-anion contacts range between 280 and 346 pm, involving O1 (3×), the central nitrogen N3 (2×) and the terminal nitrogen N2 (1×). The cation-anion assembly is characterized by four medium-strong hydrogen bonds in the range from 191 to 203 pm, where two donors are oxygen and two are nitrogen atoms (bridging and terminal) (Fig. 2).

The temperature behaviour of the lattice parameters and cell volume of ammonium cyanoureate is dis-

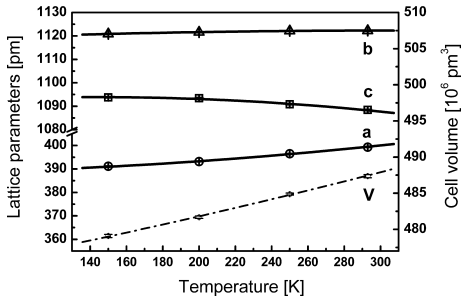

Fig. 3. Temperature dependence of the lattice parameters (left *y*-axis) and cell volume (right *y*-axis) in $NH_4[H_2NC(=O)NCN]$ as determined by X-ray powder diffraction between 150 and 293 K. The contraction of the *c*-axis with rising temperature indicates a negative thermal expansion coefficient, giving rise to an anomalous temperature behaviour.

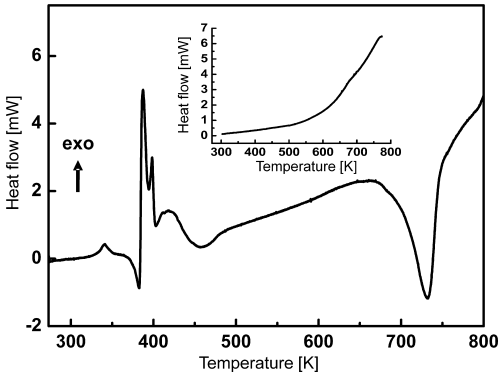

Fig. 4. DSC heating and cooling curve (inset) of $NH_4[H_2NC(=O)NCN]$ recorded between RT and 800 K with a heating (cooling) rate of 0.5 K min^{-1}.

played in Fig. 3. As evidenced by the negative slope of the curve pertaining to the crystallographic *c*-axis, the latter exhibits a negative coefficient of expansion, resulting in an anomalous thermal behaviour in the investigated temperature range. In contrast, the cell volume increases with temperature. This phenomenon is paralleled by ammonium dicyanamide [11, 12], which also exhibits a contraction of the *c*-axis with rising temperature. In spite of the formal similarity considering the symmetry and temperature characteristics of the structural parameters, the inner coordination sphere and the arrangement of the ions in the unit cells of the two structures differ. The question at issue in case of a solid-state transformation is the nature of the product determining factor, which may either be the extended solid-state arrangement of the ions as determined by the pre-organisation of the molecules in the unit cell and packing effects, or the thermodynamic driving force generating the energetically most favoured product (*i. e.* molecular structure) irrespective of the crystallographic conditions ("solution-like" conditions), or the co-action of both factors. This issue will be considered in detail in the following chapters.

Thermal analysis

Since a comprehensive description of the solid-phase reactivity of ammonium dicyanamide had been given previously [12], a comparative investigation of the thermal behaviour of the title compound seemed to be particularly intriguing. The first question that had to be addressed was whether reactivity in the solid state is likely to occur in this system, or if melting or complex decomposition are the prevailing temperature responses. As a primary step, large crystals of ammonium cyanoureate (**1**) were investigated under a microscope during thermal treatment of the sample up to 453 K. This procedure did not affect the bulk crystal shape, yet led to a continuous clouding of the initially clear crystal together with a keying of the surface and simultaneous softening of its consistency, thereby indicating the conversion into polycrystalline material or potential solid-state reactivity to occur.

DSC and DTA/TG measurements indicate significant differences in the thermal behaviour of ammonium cyanoureate depending on the heating and pressure conditions, thereby rendering the course of the thermal reactivity a complex interplay between the latter variables. The DSC curve for a sample heated continuously up to 773 K in a closed aluminium crucible (heating rate 0.5 K min^{-1}) displays a weak and broad exothermic signal at 355 K, followed by a sharp exothermic signal (onset 385 K), which is preceded in some cases by an endothermic deflection of the baseline. Between 390 and 463 K, a complex series of thermal events is observable (Fig. 4). The main product recovered after the above thermal treatment is urea together with ammeline (**6**) as proved by X-ray powder diffraction, a frequently encountered decomposition product of C-N-O materials [20, 22 – 24].

It is known from the literature that ammeline (**6**) is formed to a small extent at temperatures above 498 K as a minor decomposition product of urea besides the main products biuret (**8**), cyanuric acid, ammelide (**9**), and melamine [25]. At temperatures below 473 K, however, the formation of ammeline by urea decomposition is negligible, suggesting a different source of ammeline in the present case.

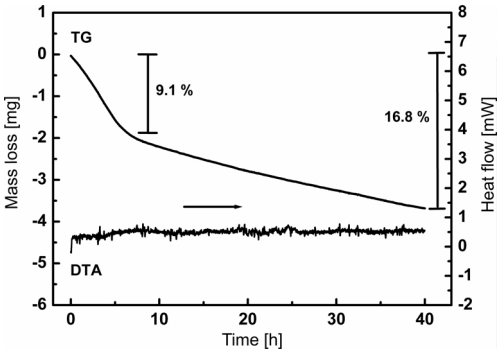

Fig. 5. Isothermal TG and DTA heating curves of $NH_4[H_2NC(=O)NCN]$ recorded at 358 K. The weight of the sample was 21.97 mg.

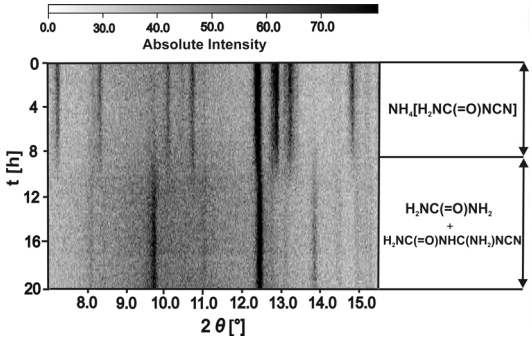

Fig. 6. Variable temperature X-ray powder diffraction patterns of $NH_4[H_2NC(=O)NCN]$ recorded at 358 K for 20 h. The measuring time for each diffractogram ($7-15.5°$ 2θ) was 11 minutes and the heating rate up to the starting temperature 5 K min^{-1}. The starting material and products are indicated at the right margin.

If the above heating experiment is conducted in an Al_2O_3 crucible open to the atmosphere (≤ 1 K min^{-1}), the products differ substantially from those obtained under DSC conditions. No ammeline formation is observed, whereas urea is detected in all product mixtures obtained below ≈ 425 K (at higher temperatures sublimation of urea occurs). Above 473 K the products are transformed into amorphous graphitic C-N materials.

If the sample is heated to 358 K (1 K min^{-1}) in unsealed Al_2O_3 crucibles and annealed for 40 h, no thermal event is recorded (DTA) in spite of the ongoing transformation of the sample as evidenced by X-ray powder diffraction. The powder pattern of the product phase recovered after 40 h is largely identical to that obtained in the heating experiments. The TG curve shows a continuous mass loss, which decreases after 5 h at 358 K where it amounts to $\approx 9.1\%$. Most likely, the observed mass loss is due to the formation of ammonia. When annealing further the curve flattens, yet the mass loss continues beyond the end of the measurement after 40 h where it has added up to 16.8% (Fig. 5).

The number of products obtained by reaction in an open system is very sensitive to only slight variations of the reaction conditions and may in the most unfavourable case lead to a complex mixture of side phases along with the main products. In the following, the thermal behaviour under optimised isothermal conditions (358 K, pressure equalisation), leading to a minimum of products, will be considered in detail.

High temperature X-ray diffraction

The *in situ* observation of the phase transformation by means of variable temperature X-ray powder diffraction further approves the absence of melting under controlled temperature conditions.

When heated isothermally at 358 K for several hours, the onset of the phase transformation is observed after 8 h (Fig. 6). As indicated by the comparatively long coexistence of the starting material and product phases (> 2 h), the reaction kinetics of the phase transformation may qualitatively be assessed as relatively slow. The transformation onset and rate increase exponentially by raising the transformation temperature, the crystallinity of the product however being correlated inversely with the annealing temperature. When compared to ammonium dicyanamide, whose optimum transformation temperature is between 368 and 373 K, the temperature characteristics for the transformation process of the two compounds is quite similar, which may suggest the ammonium ion to play a decisive role for the solid-state reactivity in both salts.

Due to the moderate crystallinity of the product phase, indexing of the powder patterns was not successful. By comparison, a part of the reflection lines could again be attributed to urea as observed in the heating experiments in a closed vessel, yet all other components could not be identified from the heterogeneous product phase by X-ray diffraction methods. Therefore, the identification of the products was attempted by complementary analytical methods, which was however complicated by the poor solubility of a large fraction of the product phase in water or organic solvents apart from DMSO.

In accord with the above observations, a series of single-crystal X-ray diffraction measurements con-

ducted isothermally at 348 – 351 K confirm the conversion of a single crystal of $NH_4[H_2NC(=O)NCN]$ into polycrystalline material after approx. 14 days. The transformation is indicated by the complete disappearance of the reflections and the emergence of Debye-Scherrer rings. The refinement of the data sets reveals the occupation factor of N1 (ammonium nitrogen) to be smaller than one ($0.89 <$ sof (N1) < 0.93), suggesting a slight tendency towards the release of ammonia without effecting a collapse of the structure. In order to fulfil the criterion of electro-neutrality, an intermolecular proton transfer to the anion must occur, leading to a small yet undetectable fraction of the free acid cyanourea, which may be incorporated statistically into the parent structure. Allowing the site occupation factor for N1 to be smaller than 1 ($\approx 0.944(6)$) for the data set collected at 140 K also slightly improved the refinement. This finding may further corroborate the occurrence of an energetically favoured static disorder due to facile proton exchange reactions in the solid state even at low temperatures, which is accompanied by the loss of small amounts of ammonia.

Vibrational spectroscopy

In accordance with the IR spectra of the transformation product the presence of urea in the product mixture is corroborated, indicated by the intense absorption lines around 1664, 1620 and 1450 cm^{-1} (Fig. 7, middle). Principally, the appearance of the product spectrum suggests the conservation of the majority of molecular fragments as compared to ammonium cyanoureate, since the presence and location of the absorption bands pertaining to the N-H, C=O and C≡N moieties are not significantly altered upon transformation.

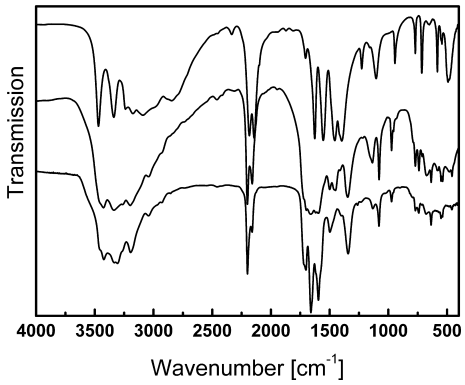

Fig. 7. IR spectra of ammonium cyanoureate (top), the decomposition product obtained at 358 K (middle) and cyanoguanylurea (bottom), recorded in a range from 4000 – 400 cm^{-1} at room temperature.

This is indicative of the core of the starting material to stay intact and, in particular, a nucleophilic attack of ammonia at the nitrile carbon as observed in ammonium dicyanamide to be most unlikely due to the still clearly visible nitrile band in the product spectrum. Owing to the product mixture and the appearance of several minor bands and band shifts, the complexity of the spectrum is increased. Among the newly emerged bands are signals at 2199 / 2159 cm^{-1} and 1703, 1499, 1346, 1136, 1079, 972, 739, 674, 635, and 458 cm^{-1}. In order to establish the identity of the missing product components, the IR data are not sufficient and need to be complemented by other spectroscopic data.

NMR spectroscopy

^1H and ^{13}C spectra of a range of products that were obtained under varying temperature conditions were recorded in DMSO-d_6 solution at ambient temperature. The ^{13}C NMR spectrum of the product obtained after optimisation of the reaction parameters, which consequently exhibits the highest degree of purity, shows three signals at 160.2, 156.0 and 116.8 ppm (Fig. 8). In some cases signals at 167.1, 158.6, and 124.3 ppm are also present, whose intensities strongly depend on the thermal history of the sample.

When the spectral region between 150 and 170 ppm is visualised enlarged, the splitting of the signal at 160 ppm becomes evident. Comparison with the

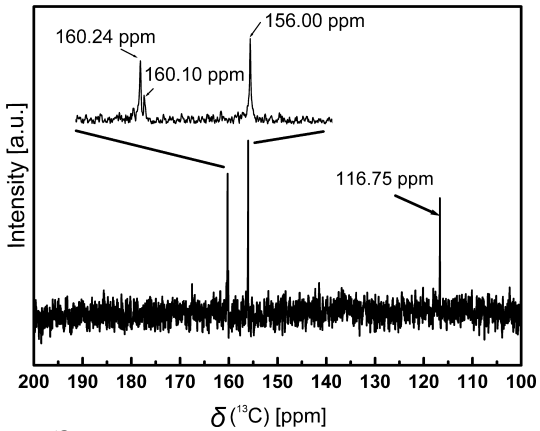

Fig. 8. ^{13}C NMR spectrum of the solid-state decomposition product of ammonium cyanoureate recorded in DMSO-d_6 solution at 293 K. The region between 150 and 163 ppm is shown enlarged in the inset.

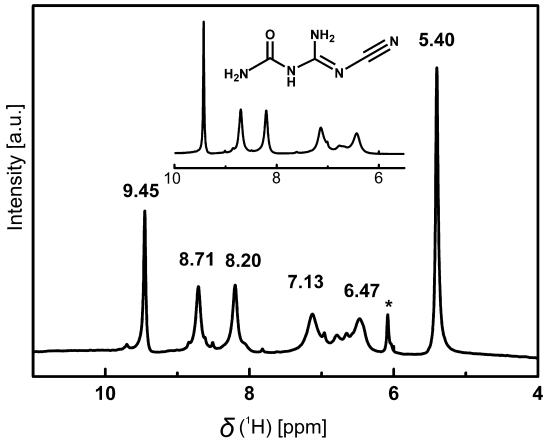

Fig. 9. ^{1}H NMR spectrum of the solid-state decomposition product of ammonium cyanoureate recorded in DMSO-d_6 solution at 293 K. The ^{1}H spectrum of cyanoguanylurea is shown in the inset; the asterisk denotes an unknown impurity.

^{13}C NMR spectrum of urea permits the assignment of one of the signals at 160 ppm to urea. The signal around 117 ppm is easily attributed to a nitrile carbon atom, whereas chemical shifts of the signals at 156, 158 and 160 ppm are characteristic of amide- or amino(imino)methyl-groups with sp^2-hybridized carbon atoms. The signals at 167 and 124 ppm are identical with the ^{13}C chemical shifts of ammonium cyanoureate, yet are also observed when no ammonium ion is detectable by ^{14}N / ^{15}N NMR spectroscopy. The ^{1}H spectrum of the product typically exhibits six signals at 5.40, 6.47, 7.13, 8.20, 8.71, 9.45 ppm and an impurity at 6.08 ppm, where the signal at 5.40 ppm can again be attributed to urea (Fig. 9). In several spectra, the signal around 7 ppm is superposed by a broad feature, indicating fast exchange of acidic N-H protons as typically observed for ammonium or guanidinium ions. Simultaneously, a medium intense signal at 5.10 ppm is present, which is close to the NH_2 protons of ammonium cyanoureate. The integrated intensities of the five major resonances, which appear in the region of both acidic and non-acidic NH and NH_2 groups, are approximately equal.

Based on the spectroscopic information sketched above the molecular structure of the missing product components may be derived:

Apart from urea, the major NMR signals indicate the formation of the isomeric urea derivatives cyanoguanylurea ([(cyanoamino)iminomethyl]-urea) (**4**, **4a**) or [N-cyanocarbamoyl]-guanidine (**11**, **11a**), which are sketched in Scheme 2. Exemplarily, two possible conformational or tautomeric isomers of each compound are shown, which are supposed to be particularly favoured energetically if intramolecular hydrogen bonding is possible ("chelate effect"). Some spectra can only be interpreted conclusively by assuming the guanidinium salt of cyanourea (**10**) to be present in the product mixture along with the above main products. Thus, the presence of the ^{13}C signals at 158 (cation), 167 and 124 ppm (anion), as well as the sharp ^{1}H signal around 5 and the broad signal at 7 ppm can be explained without invoking the presence of small portions of unreacted starting material.

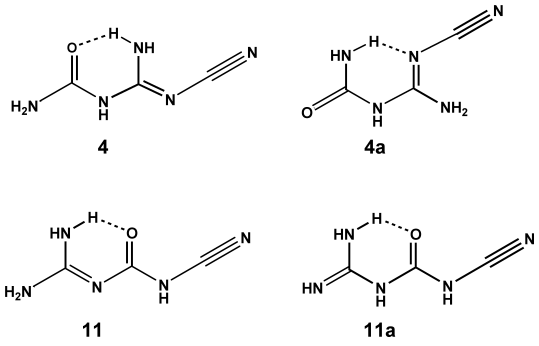

Scheme 2. Conformational isomers of cyanoguanylurea (**4**), (**4a**) and cyanocarbamoylguanidine (**11**) and (**11a**). Intramolecular hydrogen bonding is indicated by dashed lines.

Mass spectrometry

The structural picture outlined above may be corroborated by mass spectrometry. Spectra obtained by Direct Electron Ionisation (DEI+) clearly contain peaks at m/z 60 and 127, which can be assigned to the two main products urea and cyanoguanylurea (**4**) or cyanocarbamoylguanidine (**11**). The molecular peaks are supplemented by peaks at 111 $[M\text{-}NH_2]^+$, 84 $[M\text{-}HNCO]^+$, 44 $[M_{urea}\text{-}NH_2]^+$ and 43 $[M\text{-}(H_2N)_2CNCN]^+$ and $[M_{urea}\text{-}NH_3]^+$, belonging to molecular fragments of the parent mass peaks. DEI+ spectra of some decomposition products further contain weak peaks at m/z 169 and 152, which are consistent with the molecular structure of [1-cyanoguanyl-3-guanyl]urea (**12**). Although the formation of the latter as a result of thermal decomposition reactions during sample evaporation cannot be excluded, the presence of small amounts of **12** in the initial product mixture must be assumed and may be corroborated by the observation of additional NMR signals in some product samples. Some spectra exhibit signals at m/z 126

and 85, which are larger than the expected isotope peaks of 127 and 84, respectively. These peaks may be attributed to the trimerization of the intermediately formed cyanamide H_2NCN to melamine and to the corresponding decomposition products, or to the $[M\text{-}H]^+$ peak of m/z 127. No mass spectroscopic evidence is found for the formation of cyanobiuret (**5**), which was claimed to occur as a by-product in the decomposition of cyanourea in solution [20]. Mass spectra recorded in the FAB^+ mode contain a large signal at m/z 60, whereas FAB^- spectra show the presence of an anion with m/z 84. These findings are fully consistent with the assumption of guanidinium cyanoureate (m/z_{cation} 60, m/z_{anion} 84) to be formed under certain conditions as a minor conversion product.

As to the identity of the main transformation product, several reasons can be cited as evidence for cyanoguanylurea (**4**) to represent the appropriate molecular structure, yet the formation of small fractions of **11**, depending on the temperature conditions, cannot be excluded:

Foremost, the decomposition of cyanourea or a mixture of the potassium salt of cyanourea with the parent free acid in aqueous solution was reported to entail the formation of cyanoguanylurea (**4**, **4a**) as the major product [20]. In order to compare the solid-state transformation product with that obtained in aqueous solution, a mixture of ammonium cyanoureate and cyanourea in a 3:1 ratio were reacted in water at 308 K for 7 – 10 days. Both the X-ray powder pattern as well as the ^1H and ^{13}C NMR spectra of the above product correspond to those of the solid-state decomposition product, neglecting the reflections / signals due to urea present in the latter (Figs 8 and 9). Additionally, ^{15}N spectroscopic investigations of the sample synthesised according to the above procedure give strong support for the validity of structure **4**. In the proton coupled or decoupled spectra, ^{15}N signals are observed at -181.1 (s, C $\equiv$ *N*), -264.6 (s, *N*H), -278.0 (s, C=*N*), -291.2 (t, *N*H_2) and -295.3 ppm (t, *N*H_2). For structure **11** the ^{15}N signal of the bridging -NH- unit would be expected at $\delta < -300$ ppm by analogy with the related cyanourea or cyanoureate structures.

Moreover, the band location of the cyano-groups observed in the IR spectra (2200 / 2159 cm^{-1}) is very close to the nitrile signal in dicyandiamide ($(H_2N)_2C$=N-C$\equiv$N (2205 / 2165 cm^{-1}), whereas that of cyanourea ((H_2N)(O=)C-HN-C$\equiv$N is positioned at 2254 cm^{-1}, accompanied by a weak signal at 2203 cm^{-1}. The observed differences in the C$\equiv$N stretching frequencies owing to the isolobal substituents O and HN may further substantiate the validity of the cyanoguanylurea structure.

In addition, the mass spectra strongly corroborate the above conclusion by the presence of a fragment peak at m/z 84, which equals the molecular peak of dicyandiamide. The facile fragmentation of the parent peak at m/z 127 *via* a *McLafferty* type rearrangement into HNCO (m/z 43) and dicyandiamide (m/z 84) is in coincidence with the experimental pattern. The isomeric cyanocarbamoylguanidine structure (**11**, **11a**) would generate fragments with m/z 42 and 85, the latter of which however is not observed to a significant extent in the majority of the mass spectra.

Finally, the existence of cyanocarbamoylguanidine (**11**, **11a**) has not yet been established, since no data whatsoever are available on this compound in the literature. Therefore, the lack of information on the hypothetical cyanocarbamoylguanidine strongly suggests the instability of this compound, presumably with respect to the cyclisation to ammeline (**6**), which thus adds to the correctness of the above line of argument.

Discussion

The previous section has given an outline of the tentative reaction participants and characteristics, yet no conclusive picture of the reaction mechanism has been presented. This can however only be done speculatively on the argumentative basis sketched above.

In order to illuminate the potential course of the transformation, crystallographic details have to be taken into account. First of all, the product distribution strongly suggests the reaction pathway to differ substantially from that observed for ammonium dicyanamide:

Whereas in the latter case, the nucleophilic attack of the *in situ* generated ammonia occurs at the nitrile carbon atom of the dicyanamide anion, the conservation of the nitrile moiety in ammonium cyanoureate indicates the role of the ammonium group to be fundamentally different in the title compound. The evolution of ammonia appears to be more pronounced in the latter case, since it is observable by a weak exothermic event around 355 K in the DSC measurements when the sample is heated gradually. In contrast, the small mass loss due to evolving ammonia is not detectable by DSC in ammonium dicyanamide, suggesting ammonia not to be retained in the transformation products of ammonium cyanoureate stoichiometrically as is the case for

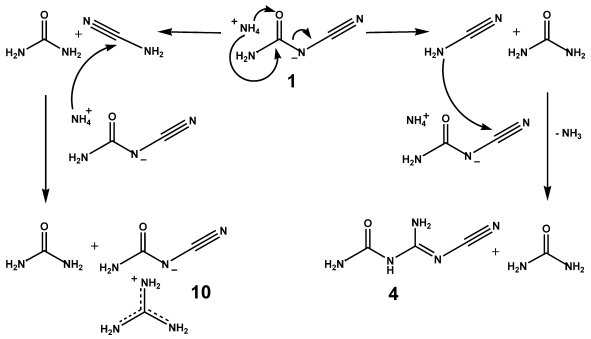

Scheme 3. Two alternative mechanistic pathways of the solid-state transformation of **1**. The two-step mechanism sketched to the right is characterized by the nucleophilic attack of the intermediately formed cyanamide at the nitrile carbon of a neighboured anion, resulting in cyanoguanylurea (**4**) and urea. The alternative pathway (left) shows the nucleophilic addition of ammonia to the cyanamide carbon C1, leading to urea and the guanidinium salt of cyanourea (**10**) without evolution of one mole ammonia.

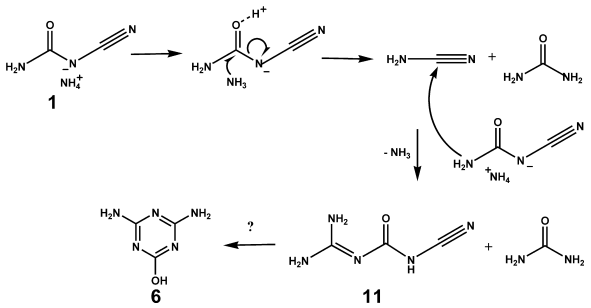

Scheme 4. Tentative reaction mechanism leading to the isomeric cyanocarbamoylguanidine (**11**) and urea by the action of the amide nitrogen of **1** as nucleophile. Subsequent cyclisation of cyanocarbamoylguanidine to ammeline (**6**) may be favoured under certain temperature conditions.

ammonium dicyanamide. As described previously, the overall assembly of the ions shows a tendency towards H···O hydrogen bonding in the present case, which is in contrast to the molecular arrangement in ammonium dicyanamide (H···N bonding) and may therefore significantly alter the solid-state reactivity as compared to the latter.

In ammonium dicyanamide, the trajectory of the protons during the transformation is directed towards the terminal and, to a lesser extent, to the central nitrogen atoms of the anion. Whereas the nucleophilic attack of the *in situ* generated ammonia can only proceed at one of the chemically equivalent electrophilic carbon atoms in ammonium dicyanamide, leading finally to the molecular compound dicyandiamide in any case,

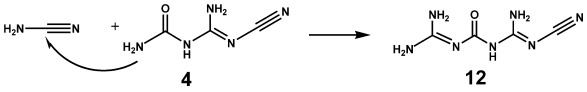

Scheme 5. Mechanism of the assumed formation of [1-cyanoguanyl-3-guanyl]urea (**12**) from cyanoguanylurea (**4**) by nucleophilic addition of the latter to the intermediately formed cyanamide.

the potential attack of ammonia in the title compound may proceed at two different carbon atoms, leading in each case to different products. The conservation of the nitrile group in one of the products suggests the attack of ammonia to take place at the carbamoyl C2 atom, thereby inducing a breakage of the C2-N3 bond and, ultimately, the generation of urea and cyanamide H_2NCN after proton exchange. The intermediately formed cyanamide is prone to consecutive reactions, such as the nucleophilic attack at a neighboured nitrile carbon to form cyanoguanylurea (**4**) (Scheme 3, right). An alternative scenario resulting in a different product distribution comes into play if ammonia is not evolved from the sample, but adds to the cyanamide intermediate to form the stable guanidinium cation, thereby blocking the nucleophilic attack of cyanamide at the parent cyanourea anion (Scheme 3, left). The spectroscopic data suggest the coexistence of both reaction pathways at low temperatures, which are realised by the different targets of the initial nucleophile ammonia. However, the significant mass loss observed in the isothermal DTA / TG experiments (first step 9.1%, final mass loss 16.8%) suggests the former reaction pathway (Scheme 3, right) to be the dominant one. Also, the observed exothermic event at 355 K in the DSC heating curve can be correlated with the evolution of ammonia, which at this stage does not induce significant structural changes as evidenced by X-ray powder diffraction. This may be assessed as further evidence for the facile release of ammonia, necessarily resulting in follow-up proton-transfer reactions. In a consecutive reaction, the main product cyanoguanylurea may further act as a nucleophile, attacking the intermediate cyanamide to form [1-cyanoguanyl-3-guanyl]urea (**12**), which is detected as a side phase by mass spectrometry (Scheme 5).

Since the reaction sequence leading to the observed products proceeds in the solid state and, hence, is dominated by little molecular freedom, the pre-orientation of the reactive centres is assumed to be such that the diffusion length necessary for the reaction to occur is minimised. Taking into account the thermal behaviour

of the lattice parameters, a competing reaction pathway may become increasingly favoured. Since the anions are arranged in a head-to-tail manner along [001], the amide group of one anion is located close to the nitrile moiety of a neighboured anion (N4···C1 355 pm at 140 K) (Fig. 1). Owing to the anomalous contraction of the *c*-axis with rising temperature, the reactive centres move closer and a nucleophilic attack of the amide N4 at C1 prior to or after breakage of the C2-N3 bond would lead to the isomeric cyanocarbamoylguanidine structure (**11**) as sketched in Scheme 4.

Although this reaction pathway seems to be facile in terms of the structural arrangement, no evidence has been found for the formation of **11** as discussed above. It may however not be excluded that under certain reaction conditions the formation of this isomer **11** is favoured, presumably followed by rapid cyclisation to ammeline, which is found as the major product in the DSC experiments (Scheme 4).

Conclusion

The novel compound ammonium cyanoureate has been synthesised and characterized by single-crystal X-ray diffraction and its solid-state decomposition elucidated with respect to the principle intermediates and reaction products. The thermal behaviour was found to be very sensitive to the temperature conditions and may yield a complex mixture of products owing to several competing reaction pathways. Whereas in a closed system the formation of urea and ammeline is favoured beyond 410 K, under optimised conditions at 358 K cyanoguanylurea has been identified as a main product besides urea. The detection of the guanidinium salt of cyanourea in varying amounts depending on the reaction conditions corroborates the formation of cyanamide as a reaction intermediate. In spite of its complexity, the transformation proceeds in the solid phase, resulting in a microcrystalline mixture of the reaction products. Thus, the thermal reactivity of ammonium cyanoureate fundamentally differs from the related compound ammonium dicyanamide which may tentatively be correlated with the differing hydrogen bonding network, resulting in a more facile release of ammonia, and the altered reactivity of the anion due to the presence of an electrophilic amide carbon. The above example further demonstrates the interplay between the chemical functionality and the reaction conditions, leading to a variety of possible reaction pathways different from those in solution, which are not significantly limited by the rigid crystal lattice.

Experimental Section

Synthesis

Ammonium cyanoureate was synthesised by neutralisation of the free acid cyanourea with aqueous ammonia. Typically, to 500 mg (5.9 mmol) cyanourea were added 1 – 3 ml (13.3 mmol) conc. NH_3 solution (Merck, 25%) and the white suspension dissolved in 12 ml water (pH = 9 – 10) and stirred for one hour. Afterwards the solution is filtered and left for crystallisation by slow evaporation. Cyanourea was synthesised by loading 8.0 g (50.6 mmol) urea-phosphate (Fluka, $\geq$ 98%) on a strongly acidic ion exchange resin (Merck, Ionenaustauscher I, H^+-Form, Art. 4765), washing the resin with 1.0 l water and pouring a solution of 1.0 g (11.2 mmol) sodium dicyanamide $Na[N(CN)_2]$] (Fluka, $\geq$ 96%, 0.5 M) onto the column. As a result, the dicyanamide is converted into cyanourea by acid hydrolysis without ion exchange taking place. A more convenient and direct synthesis for cyanourea, however, is the alkaline hydrolysis of dicyandiamide in boiling 3N NaOH solution for 2 hours, which is described in detail elsewhere [24, 26]. ^{1}H NMR (400.0 MHz, DMSO-d_6): $\delta = 7.2$ (s, 4H, NH_4), 5.3 (s, 2H, NH_2). – ^{13}C{^{1}H} NMR (100.5 MHz, DMSO-d_6): $\delta = 123.5$ ($C \equiv$N), 167.0 (C=O). MS (FAB$^-$, 6 kV): $m/z(\%) = 84$ (11) $[H_2NC(=O)NCN^-]$.

Cyanoguanylurea was synthesised according to the procedure described in [20] by constantly stirring 706 mg (6.9 mmol) of ammonium cyanoureate with 196 mg (2.3 mmol) of cyanourea in 15 ml water at 308 K. After 3 – 4 days, the white product started to precipitate, yet the reaction was maintained for another 4 – 5 days and the insoluble product isolated by filtration. In order to increase the yield, 100 mg cyanourea was added to the filtrate and the mixture again subjected the above reaction conditions.

The thermal conversion of ammonium cyanoureate was either effected under "DSC conditions" as described in the *Thermal analysis* section, or probed by heating the sample, which was placed in an unsealed Al_2O_3 crucible contained in a glass tube, with 1 K min^{-1} from 293 K to various temperatures between 400 and 463 K under pressure equalisation ("DTA conditions"). Isothermal measurements were typically conducted under the same conditions using target temperatures between 358 and 368 K. The annealing time ranged between 20 and 60 h.

X-ray diffraction

X-ray diffraction data of a $NH_4[H_2NC(=O)NCN]$ single crystal were collected at 140 K and between 343 and 351 K (high temperature measurements) on a four-circle

diffractometer (STOE Stadi 4) equipped with a 600 Series Cryostream Cooler (Oxford Cryosystems), using graphite monochromated Mo-K_α radiation ($\lambda = 71.073$ pm). The starting temperature for the high temperature measurements was adjusted by applying heating rates of approx. 1 K min^{-1}. The crystal structure was solved by direct methods employing the program SHELXTS-97 [27] and refined on F^2 using the full-matrix least-squares method implemented in SHELXTL-97 [28]. A semi-empirical absorption correction based on psi-scans was applied. The positions of all hydrogen atoms could be determined unequivocally from difference Fourier syntheses and all non-hydrogen atoms were refined anisotropically. Details of the structure determination and crystallographic data are summarised in Table 1. Intramolecular distances and angles are listed in Table 2. Further details of the crystal structure investigation are available from the Fachinformationszentrum Karlsruhe, D-76344 Eggenstein-Leopoldshafen (Germany), on quoting the depository number CSD-414279, the name of the authors, and citation of the paper.

High temperature *in situ* X-ray diffractometry was performed on a STOE Stadi P powder diffractometer (Ge(111)-monochromated Mo-$K_{\alpha 1}$ radiation, $\lambda = 70.093$ pm), with an integrated furnace using unsealed quartz capillaries. The data collection was restricted to a 2θ range of $7 - 15.5^\circ$ and a single scan collection time of 11 minutes. The sample was heated up to the starting temperature (358 K) by applying a heating rate of 5 K min^{-1} and subsequently tempered for 20 h.

Vibrational spectroscopy

FTIR measurements were carried out on a Bruker IFS 66v/S spectrometer scanning a range from 400 to 4000 cm^{-1}. The samples were prepared as a KBr pellet (5 mg sample, 500 mg KBr) under atmospheric conditions.

Thermal analysis

Thermoanalytical measurements were conducted between RT and 573 K on a Mettler DSC 25 applying a heating rate of 0.5 or 1 K min^{-1}. The alumina crucibles used as sample containers were placed in the calorimeter under an atmosphere of dry nitrogen.

For combined DTA/TG measurements at 358 K using a heating ramp of 0.5 or 1 K min^{-1} a Setaram thermoanalyser TGA 92-2400 was available. The samples were placed in an unsealed Al_2O_3 crucible and the measurements conducted under nitrogen.

General methods

^1H and ^{13}C NMR spectra were recorded as DMSO-d_6 solutions on a JEOL Eclipse EX-400 instrument, the chemical shifts being referenced with respect to TMS.

Mass spectra were obtained using a Jeol MStation JMS-700 gas inlet system. The substances were dissolved in a 3-nitrobenzyl alcohol matrix (FAB^-, FAB^+) on a target and ionized by bombardment with accelerated (6 kV) Xe atoms. For direct insertion probes using DEI+ (70 eV), the sample was suspended in MeOH and heated rapidly on a platinum filament.

Acknowledgements

The authors thank Dipl.-Chem. J. Weigand for the donation of cyanourea, A. Lieb and Dipl.-Chem. U. Baisch for the single-crystal data collection, W. Wünschheim and Dipl.-Min. S. Schmid for conducting the DSC and DTA/TG measurements, Dr. G. Fischer and D. Ewald, as well as Priv.-Doz. Dr. K. Karaghiosoff for carrying out the mass spectrometric and NMR measurements, respectively. Financial support from the Fonds der Chemischen Industrie (scholarship for B. V. Lotsch) and the Deutsche Forschungsgemeinschaft is gratefully acknowledged.

[1] J. Shorter, Chem. Soc. Rev. **7**, 1 (1978).
[2] J. D. Dunitz, K. D. M. Harris, R. L. Johnston, B. M. Kariuki, E. J. MacLean, K. Psallidas, W. B. Schweizer, R. R. Tykwinski, J. Am. Chem. Soc. **120**, 13274 (1998).
[3] C. A. Tsipis, P. A. Karipidis, J. Am. Chem. Soc. **125**, 2307 (2003).
[4] F. Toda, Organic Solid-State Reactions, Kluwer Academic Publishers, Dordrecht (2002).
[5] A. P. Purdy, E. House, C. F. George, Polyhedron **16**, 3671 (1997).
[6] E. Irran, B. Jürgens, W. Schnick, Chem. Eur. J. **7**, 5372 (2001).
[7] B. Jürgens, E. Irran, J. Schneider, W. Schnick, Inorg. Chem. **39**, 665 (2000).
[8] B. Jürgens, E. Irran, W. Schnick, J. Solid State Chem. **157**, 241 (2001).
[9] W. Madelung, E. Kern, Liebigs Ann. Chem. **427**, 1 (1922).
[10] B. Jürgens, H. A. Höppe, E. Irran, W. Schnick, Inorg. Chem. **41**, 4849 (2002).
[11] B. V. Lotsch, J. Senker, W. Kockelmann, W. Schnick, J. Solid State Chem. **176**, 180 (2003).
[12] B. V. Lotsch, J. Senker, W. Schnick, Inorg. Chem. **43**, 895 (2004).
[13] F. Hallwachs, Liebigs Ann. Chem. **153**, 293 (1870).
[14] Yu. I. Mushkin, A. I. Finkel'shtein, Russ. J. Gen. Chem. **33**, 1883 (1963).
[15] J. S. Blair, G. E. P. Smith, J. Am. Chem. Soc. **56**, 907 (1934).

[16] H. Beyer, H. Schilling, Z. Chem. **5**, 182 (1965).
[17] H. Beyer, H. Schilling, Chem. Ber. **99**, 2110 (1966).
[18] D. Britton, Acta Crystallogr. **C43**, 2442 (1987).
[19] N. S. Magomedova, Z. V. Zvonkova, Zh. Strukt. Khim. **15**, 165 (1974).
[20] K. Iio, Bull. Chem. Soc. Jpn. **57**, 625 (1984).
[21] Yu. I. Mushkin, A. I. Finkel'shtein, Kinet. Katal. **7**, 219 (1966).
[22] Yu. I. Mushkin, A. I. Finkel'shtein, Zh. Org. Kh. **3**, 507 (1967).
[23] H. Beyer, Z. Chem. **6**, 213 (1966).
[24] H. Bieling, P. Barth, H. Beyer, Z. Chem. **4**, 146 (1964).
[25] P. M. Schaber, J. Colson, S. Higgins, E. Dietz, D. Thielen, B. Anspach, J. Brauer, American Laboratory **31**, 13 (1999).
[26] H. Beyer, Z. Chem. **6**, 213 (1966).
[27] G. M. Sheldrick, SHELXS97, Program for the Solution of Crystal Structures, University of Göttingen (1997).
[28] G. M. Sheldrick, SHELXL97, Program for the Refinement of Crystal Structures, University of Göttingen (1997).